







Article

# Multidisciplinary Laser Facility Driven by New-Generation High-Repetition Laser

Gonçalo Vaz <sup>1</sup>, Joana Alves <sup>1,2</sup>, Victor Hariton <sup>1,3</sup>, Celso P. João <sup>1,4</sup>, João Marques <sup>1</sup>, David Cristino <sup>1</sup>, Hugo Gomes <sup>1</sup>, Cara Priebe <sup>5</sup>, Petr Pokorny <sup>6</sup>, Maria P. Santos <sup>1</sup>, Hugo Pires <sup>1,\*</sup> and Gonçalo Figueira <sup>1</sup>

<sup>1</sup> GoLP/Instituto de Plasmas e Fusão Nuclear, Instituto Superior Técnico, Universidade de Lisboa, 1049-001 Lisbon, Portugal; gonalovaz98@tecnico.ulisboa.pt (G.V.); silveira.marques@tecnico.ulisboa.pt (J.M.); david.cristino@tecnico.ulisboa.pt (D.C.); hugo.c.gomes@tecnico.ulisboa.pt (H.G.)

<sup>2</sup> NKT Photonics A/S, Bregnerødvej 144, 3460 Birkerød, Denmark

<sup>3</sup> Deutsches Elektronen-Synchrotron DESY, Notkestraße 85, 22607 Hamburg, Germany

<sup>4</sup> LaserLeap Technologies, Rua Coronel Júlio Veiga Simão, CTCV Edifício B, 3025-307 Coimbra, Portugal

<sup>5</sup> Technische Hochschule Luebeck, Moenkhofer Weg 239, 23562 Luebeck, Germany

<sup>6</sup> Faculty of Nuclear Sciences and Physical Engineering, Czech Technical University in Prague, Břehová 7, 115 19 Prague, Czech Republic

\* Correspondence: hugo.pires@tecnico.ulisboa.pt

**Abstract:** For many years, high-power laser technology has been divided between industrial applications, which prioritize higher average powers and repetition rates, and academic research, which focuses on achieving higher peak powers and ultrashort pulse durations. The introduction of Yb-doped crystals in laser technology has paved the way for a new generation of laser sources that bridge the gap between industrial and academic requirements, combining high average power with ultrashort pulse capabilities. These advancements enable the integration of compact, adaptable front-end stages, making such lasers versatile for scientific applications. In Lisbon, the Laboratory of Intense Lasers leverages this technology with a system that combines commercial and custom-built front-end stages to enhance operational flexibility. In this paper, we present the current status of this facility and outline upcoming upgrades. We also showcase applications enabled by these high-power laser sources, including semiconductor studies, bi-photonics, and time-resolved spectroscopy.

**Keywords:** ultrafast laser and applications; frequency conversion; laser amplifiers; multipass cell; pulse compression; nonlinear optics; mid-infrared; laser facility; high-repetition rate



**Citation:** Vaz, G.; Alves, J.; Hariton, V.; João, C.P.; Marques, J.; Cristino, D.; Gomes, H.; Priebe, C.; Pokorny, P.; Santos, M.P.; et al. Multidisciplinary Laser Facility Driven by New-Generation High-Repetition Laser. *Photonics* **2024**, *11*, 1157. <https://doi.org/10.3390/photonics11121157>

Received: 31 October 2024

Revised: 26 November 2024

Accepted: 27 November 2024

Published: 9 December 2024



**Copyright:** © 2024 by the authors. Licensee MDPI, Basel, Switzerland. This article is an open access article distributed under the terms and conditions of the Creative Commons Attribution (CC BY) license (<https://creativecommons.org/licenses/by/4.0/>).

## 1. Introduction

Ultrafast, high-power lasers have transformed modern science, enabling groundbreaking research across a wide range of disciplines, from physics and chemistry to biology and materials engineering. The progress in this field has been largely driven by the development of Chirped Pulse Amplification (CPA) [1], a concept that allows for the amplification of femtosecond pulses to high energies without damaging the amplification medium and that has become cornerstone technology in ultrafast laser systems. Building on CPA technology, further advancements were achieved with Optical Parametric Chirped Pulse Amplification (OPCPA) [2–5], which combines the pulse stretching of CPA with optical parametric amplification, allowing for tunable output across a range of wavelengths as well as better control over pulse duration. With OPCPA, researchers can access wavelengths beyond the traditional gain bandwidth of laser crystals, expanding the scope of ultrafast experiments to previously inaccessible spectral regions. Thanks to these advancements, many modern laser facilities now house a diverse array of laser systems with the capability to deliver high peak powers, broad wavelength tunability, and femtosecond to attosecond pulses. This versatility supports a wide range of cutting-edge experiments in nonlinear optics, strong-field physics, particle acceleration, and materials processing. The availability

of ultrashort, high-intensity pulses has opened up new experimental regimes, allowing scientists to explore phenomena such as high-harmonic generation, relativistic electron dynamics, and laser-driven particle acceleration [5]. A recent trend within these facilities is the adoption of industrial-grade, diode-pumped Yb-lasers. Yb-based lasers, with their high efficiency, stability, and scalability, are an ideal choice for research requiring high average power with excellent beam quality. Traditionally used in industrial settings, high-power, high-repetition-rate Yb-lasers are being increasingly introduced into laboratory environments, where they are increasingly paired with CPA and OPCPA stages to enhance both energy and versatility. This integration represents a shift towards what has been termed the “third generation” of femtosecond laser technology [6], characterized by the marriage of industrial reliability with the ultrashort-pulse capability required for scientific applications. The Laboratory of Intense Lasers (L2I) is a laser facility located at the Instituto Superior Técnico, University of Lisbon. Operating since 1998, it has been devoted to the development of high-intensity lasers, ultrashort diagnostics, and high-intensity interactions such as particle acceleration, high-harmonic generation, and advanced radiation sources [7].

L2I has undergone a series of major upgrades over the past few years, envisioning high-repetition-rate operation, including a new 100 W, 100 kHz, 1 ps industrial-scale Yb:YAG laser. These short durations (and consequently higher peak powers) allow for the assembly of relatively compact nonlinear stages, while the high energies help compensate for the inherent low conversion efficiencies of the nonlinear processes.

This laser drives a multipass-cell (MPC) compressor to generate sub  $\sim 100$  fs 1030 nm pulses and a state-of-the-art OPCPA operating at 3000 nm. Collectively, these systems enable a range of parameters applicable to a plethora of scientific disciplines deriving from a single laser source.

In this paper, we report how a single laser source can drive the current capabilities of the L2I as a high-power, ultrashort laser facility. We start with a description of our laser source and the current nonlinear stages utilized to adapt/improve its parameters, together with the incoming upgrades to these systems further expanding the parameter range. Finally, we present some of our early experimental results.

## 2. Laser System Setup

The setup of the current L2I laser system, together with planned upgrades currently under development (dashed boxes), is shown in Figure 1.

### 2.1. Main Driving Laser

The full system is driven by a high-average-power, high-repetition-rate, diode-pumped Yb:YAG InnoSlab amplifier (AMPHOS, A2000), delivering 1 ps, 1 mJ pulses centred at 1030 nm and an adjustable repetition rate between 0.1 and 40 MHz. At the standard repetition rate of 100 kHz, the average output power is 100 W. The spectrum and Frequency-Resolved Optical Gating (FROG) trace of this system can be seen in Figure 2 and Figure 3, respectively.

At the output of this laser, a polarizer (PL1) and a half-wave plate split the beam in two. The primary output (about 75% of the energy) is used to seed a mid-infrared OPCPA, with the remaining fraction being reserved for other applications such as pulse compression or further amplification at 1  $\mu\text{m}$ .

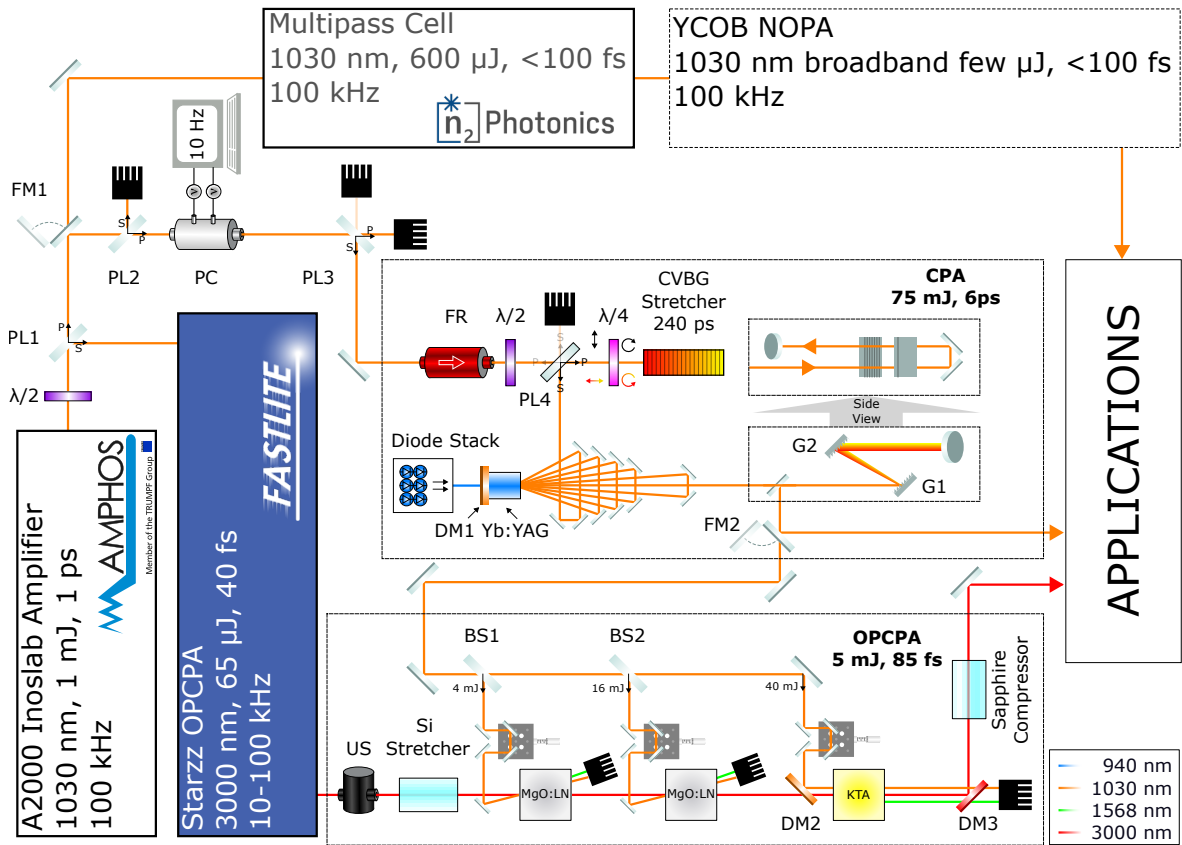


**Figure 1.** Schematic of the laser capabilities at the L2I facility. The CPA, NOPA, and 5 mJ OPCPA systems are currently under development. The current progress of the NOPA system can be seen in Section 2.5.  $\lambda/2$ : half-wave plates;  $\lambda/4$ : quarter-wave plates; PL1-4: polarizers; FM1-2: flip mirrors; BS1-2: beam splitters; DM1-2: dichroic mirrors; PC: Pockels cell; FR: Faraday rotator; CVBG: chirped volume Bragg grating; G1-2: diffraction gratings; US: ultrafast shutter.

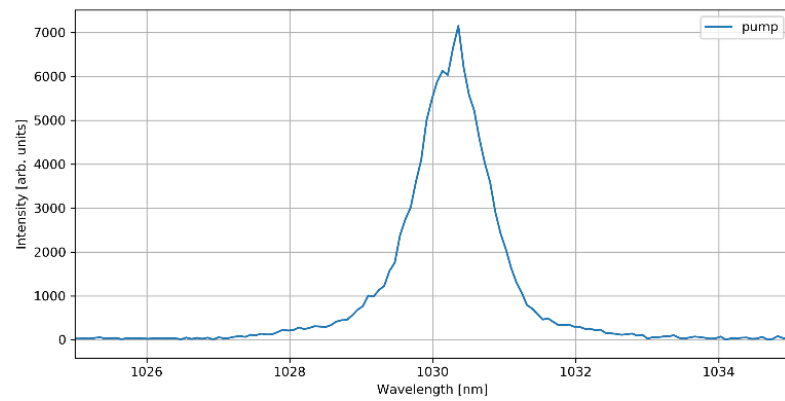


**Figure 2.** Output spectrum of the A2000 system.

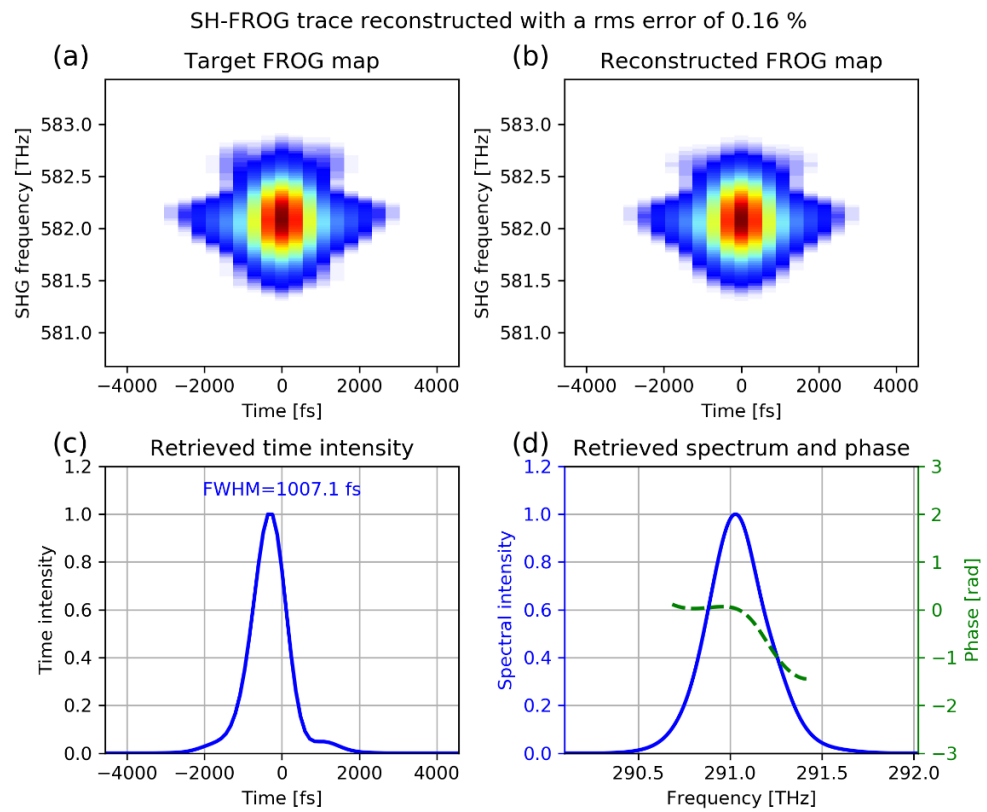


**Figure 3.** FROG measurement of the shortest possible pulses generated by the A2000 system.

### 2.2. Mid-Infrared OPCPA

The mid-infrared OPCPA (Starzz, FASTLITE) is optimized to match the output of the pump system, generating 40 fs, 65  $\mu$ J, carrier-envelope phase (CEP) stable pulses centred at 3000 nm and at the pump repetition rate of 100 kHz. The amplifier is a virtually passive device, with the only active components (excluding diagnostics) being a pair of motorized mirrors for pointing correction of the input, and an ultrafast acousto-optic programmable dispersive filter (Dazzler, Fastlite) for CEP control. The architecture of this system is mostly similar to that of [8]. The output spectrum and FROG trace of this system can be seen in Figure 4 and Figure 5, respectively. The FWHM spectral bandwidth is 16.1 THz, with a corresponding time-bandwidth product of 0.63.

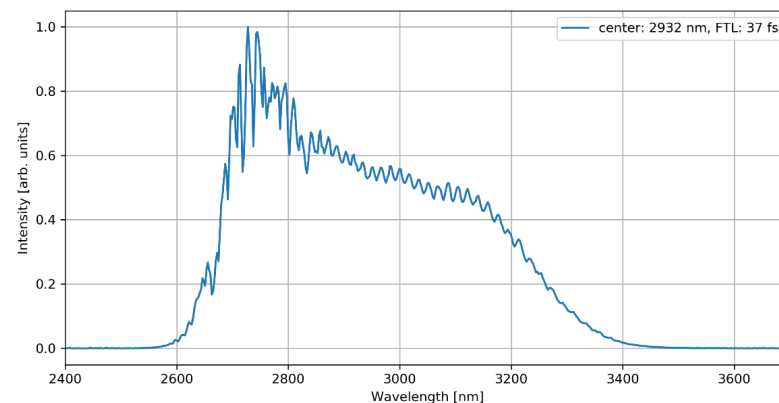


**Figure 4.** Output spectrum of the mid-IR OPCPA.

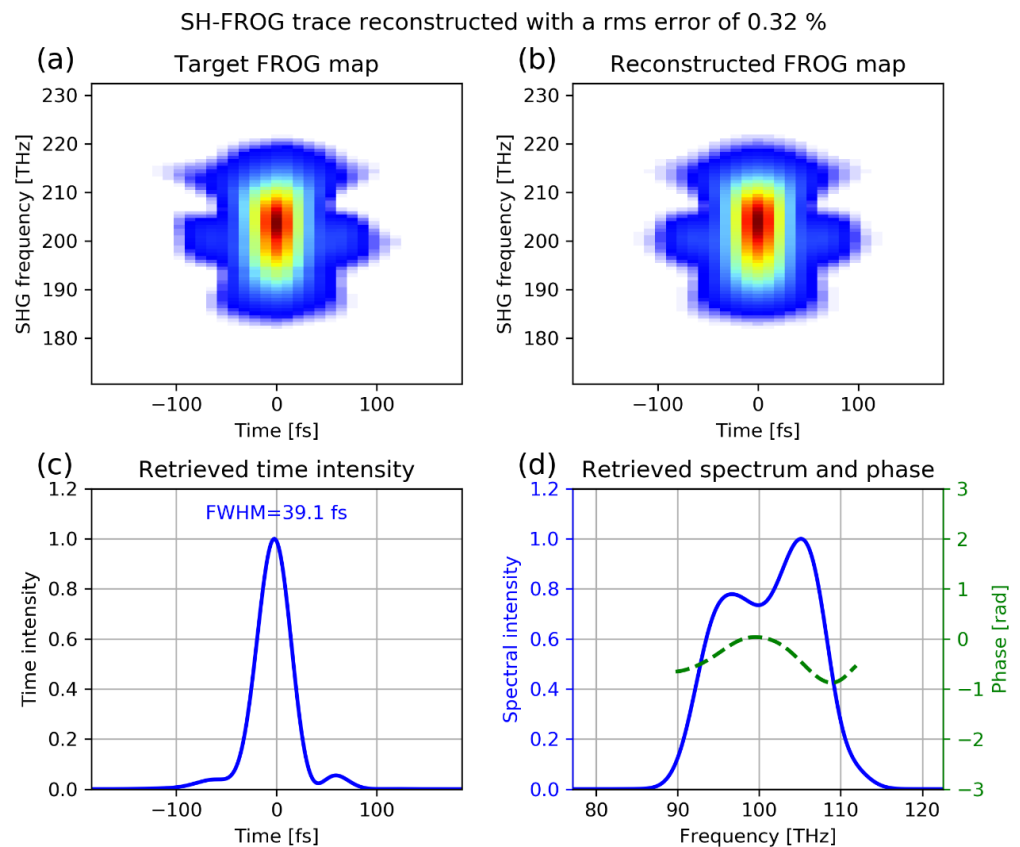


**Figure 5.** FROG measurement of the pulses generated by the mid-IR OPCPA system.

The operating parameters of the OPCPA system make it one of a selected few at a worldwide level capable of addressing challenging applications ranging from strong-field physics and attosecond science to pollutant tagging and cancer diagnostics [9,10].

### 2.3. Multipass Pulse Compression

Multipass pulse compression [11–13] has become increasingly important in ultrafast laser systems thanks to its ability to generate high-energy, ultrashort laser pulses with high precision. This technique involves multiple passes of a laser pulse through a nonlinear medium (gas or solid) with dispersion compensation, allowing it to compress the pulse duration progressively without compromising its energy, making it a key enabler for multiple applications. Recent advances in optical materials, dispersion control, and nonlinear compression techniques have significantly improved the efficiency and reliability of multipass pulse compression, allowing for more compact and robust laser systems [11–13]. Our MPC [14] was developed through a partnership with n2-Photonics and a similar model is now commercially available. The system consists of a Herriot cell composed of two parallel concave mirrors placed inside a gas chamber filled with pressurized noble gas (currently krypton at 3 bar). Pulses are injected into the cell and undergo multiple reflections between the mirrors. As they pass through the focal region, the high intensities lead to self-phase modulation (SPM) and spectral broadening. The output pulses are compressed by a pair of chirped mirrors. The MPC system can be used with an input energy up to 0.75 mJ, in which case the 1 ps pulses are compressed to below 100 fs with an efficiency of 85% while preserving or even improving the spatial profile quality. The highest compression ratio obtained with this system can be seen in Figure 6.

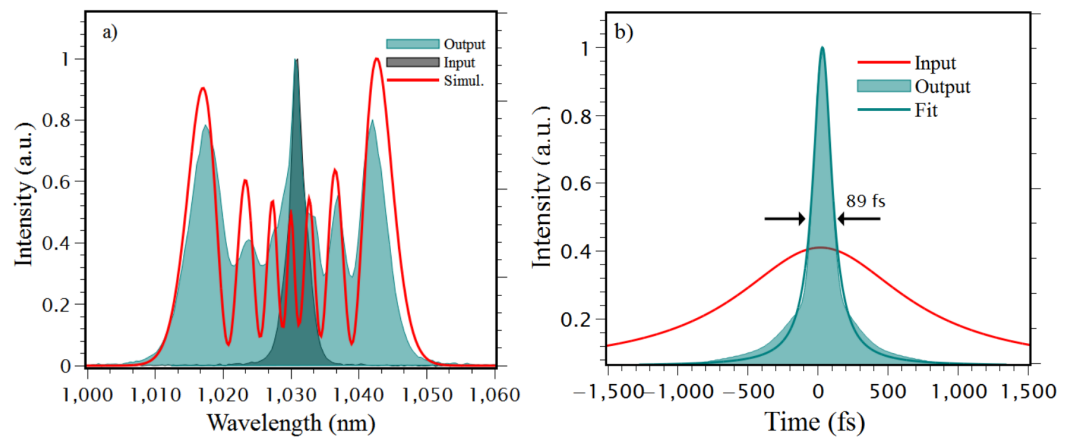


**Figure 6.** (a) Input (dark green area) and output (light green area) pulse spectrum for 1 mJ input energy using 3 bar of krypton inside the MPC. The red line shows the corresponding simulation. (b) Input (red line) and output (green area) pulse profile, together with Gaussian fit (green line). The FWHM pulse duration is 89 fs with a Fourier-transform limit of 82 fs. From Ref. [14].

As the broadening is driven by SPM, the compression ratio can be adjusted by the input power of the laser. Since many applications require the attenuation of the output, the interplay between input power and attenuation allow the running of experiments at the same energy/power levels while scanning the effects of pulse duration. This system is also fully passive and the gas chamber is able to keep the high pressure for several months without any gas intake. The output of the MPC drives several user experiments, taking advantage of the higher peak powers, shorter temporal resolution, and broader spectrum, as described in Section 3.1.

#### 2.4. Millijoule OPCPA Stage

Many experiments benefit from higher pulse energies in the mJ-range, including strong-field ionization and high-harmonic generation, molecular spectroscopy and dynamics, and plasma physics. For these goals, we have designed an additional ultra-broadband OPCPA, envisaging >mJ-level, sub-50 fs pulses in the 3  $\mu\text{m}$  region. The design relies on amplifying the secondary output of the A2000 in a home-built chirped pulse amplifier (Figure 1) to act as a pump, and stretching the output to the mid-infrared system for the signal. The output beam from the A2000 is redirected to this system by flipping an adjustable mirror mount (FM1). To reduce the damage threshold requirements and prevent depopulation of the gain medium in the CPA, at this stage, the repetition rate of the pulse train is lowered to 10 Hz with a pulse-picker, consisting of a Pockels cell (PC) (cell by Leysop, driver by BME), synchronized with the A2000 internal trigger, mounted between two crossed polarizers (PL2 and PL3). A Faraday rotator (FR) further prevents any back reflection into the driving laser. The beam is sent to a compact stretcher consisting of 33 mm long, 5  $\times$  8 mm aperture, 26 ps/nm chirped volume Bragg grating (CVBG) (Optigrade) that increases the pulse duration from 1 ps to 240 ps. The stretched pulse is sent into a diode-pumped multipass amplifier (see Refs. [7,15] for details). The pulse passes 10 times through an 8 mm thick Yb:YAG crystal pumped by a 4 kW laser diode stack operating at 940 nm (Jenoptik). The pump radiation goes through a dichroic mirror (DM1) next to the gain crystal that is transmissive for the 940 nm pump but highly reflective at 1030 nm. This amplifier has been demonstrated to reach 100 mJ per pulse with a  $\sim$ 140 ps pulse duration. Compression will be performed with a compact Treacy compressor composed of two parallel diffraction gratings (G1 and G2), with an expected output of 75 mJ, 6 ps pulses at 10 Hz. Since the pump and signal pulses will be synchronised optically, minimizing the optical path of this system is crucial to avoid the need for long delay lines. With this upgrade, we aim to have two laser systems operating at 1030 nm: a moderate-energy, high-

repetition-rate one for low-cross-section interactions and a high-energy, low-repetition-rate one for low-efficiency phenomena.

The in-house built, mid-infrared OPCPA system is designed to operate at 3000 nm [16,17]. The repetition rate of the Fastlite system will be matched to the 10 Hz of the pump by first internally reducing the repetition rate to 1 kHz, followed by an ultrafast shutter/chopper (US). The 40 fs pulses will be stretched up to 2 ps in a silicon slab. This corresponds to one-third of the pump pulse duration to ensure amplification without bandwidth narrowing. The OPCPA system is composed of three amplification stages, the first two based on MgO:LN in a noncollinear configuration, ensuring broadband amplification, and the third one a collinear stage based on KTA crystal to achieve higher gain. The pump is split (BS1,BS2) for the three stages at a ratio of 4 mJ/16 mJ/40 mJ, with independent delay lines to allow for synchronization. The collinearity of the KTA stage has an expected OPCPA efficiency of 8%, and the amplifier is designed to reach the 5 mJ level. This system was designed to use only 60 out of the 75 mJ available for pumping, to account for any unexpected losses or underperformance of the previous systems, leaving also the possibility of further amplification with a fourth stage. Finally, the amplified pulses are sent to a bulk sapphire compressor resulting in a 5 mJ, 85 fs output. The Fourier limit is close to the original 40 fs of the Starzz system; however, simulations with a simple bulk compressor demonstrate some uncompensated third-order dispersion. This could be corrected with a prism pair compressor or an acousto-optic modulator, albeit at the cost of energy.

### 2.5. YCOB-Based NOPA

The last laser source is a noncollinear optical parametric amplifier (NOPA) based on the nonlinear crystal yttrium calcium oxyborate (YCOB) and operating around 850 nm. This source builds on a previously demonstrated NOPA capable of generating microjoule-level broadband (ranging from 750 to 950 nm) short pulses [18–20]. The output of the MPC stage is used as the driver of this system with the goal of generating high-intensity broadband laser pulses (Figure 7). The 1030 nm pulse train is split into two beamlines at a thin film polariser (TFP). The signal beam line is focused on a sapphire plate for generating supercontinuum, to be used as the signal. The pump beamline is sent through a BBO crystal for second-harmonic generation and separated from the fundamental in a dichroic mirror (DM). Both beams are sent into the NOPA consisting of a 7.5 mm thick YCOB crystal, with an auxiliary delay stage for temporal synchronization. Due to the shorter output pulse duration enabled by the MPC, a broad supercontinuum is generated, motivating the choice of a NOPA geometry. It is also important to note that YCOB is a biaxial crystal and that the phase matching and noncollinear angles were thoroughly modelled and chosen outside the principal planes to enable maximum broadband capability [18,19,21]. The output spectrum is capable of supporting a compressed pulse duration of 30 fs. Finally, pulse compression will be performed via a prism pair compressor and/or a grating Treacy compressor, assisted by chirped mirrors if required.

Table 1 summarises the laser systems at L2I, both operational and under development.

**Table 1.** Current and future laser capabilities of the L2I.

Parameter \ System	NIR 100 kHz	MPC	Mid-IR OPCPA	YCOB OPA *	CPA *	3OPA *
Wavelength (nm)	1030	1030	3000	1030	1030	3000
Energy (μJ)	1000	600	65	1–10	75,000	5000
Duration (fs)	1000	<100	40	<100	6000	85
Rep. rate (kHz)	100	100	100	100	0.01	0.01

\* Under development.

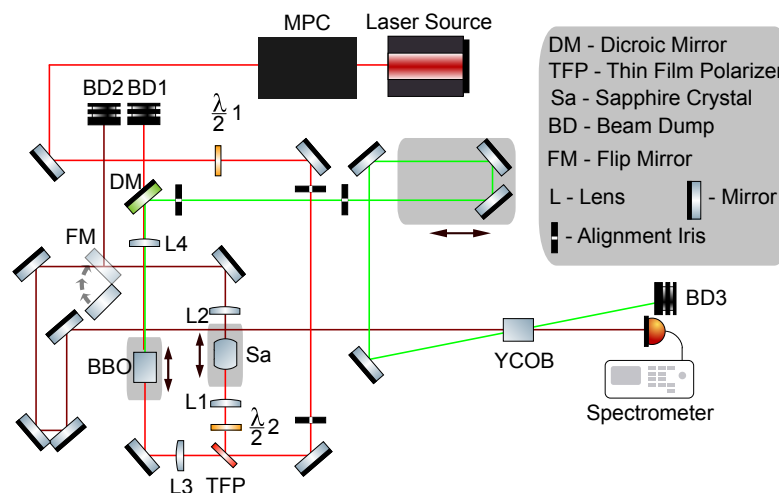


Figure 7. Schematic of YCOB-based NOPA.

### 3. Applications

In this section, we summarise some of the applications demonstrated with the current capabilities of L2I.

#### 3.1. Near-Infrared Studies

The following experiments were driven at 1030 nm by the output of the MPC. The advantages of using this system with regard to the A2000 include larger spectral bandwidth, shorter durations, and higher peak powers.

##### 3.1.1. Material Study and Characterization

In solids, the process of harmonic generation has a contribution from the bulk medium and another from the entry and exit surfaces. Typically, the contribution from the medium is many times larger than that from the surfaces due to the greater interaction length. However, in centrosymmetric media (i.e. media possessing inversion symmetry), even order processes are only possible at the surfaces, where the symmetry is broken in the normal axis [22–24]. This research line (Figure 8) aims to characterize the ultrafast laser light response of several material surfaces using the spectrum of the emitted radiation in a reflective configuration. The pulse duration is controlled by adjusting the power input into the MPC. A half-wave plate and polarizing beamsplitter cube (BSC1) are used to select the desired energy. The position of lens L1 adjusts the beam spot size on the sample, which is measured using a CMOS sensor at the same distance from the lens as the sample. After interaction, the beam is re-collimated by lens L2. The polarization of the incident beam is set by a second  $\lambda/2$ , and the sample holder allows for the precise rotation of the sample along its surface normal. The P and S components of the polarization are separated using another polarizing beamsplitter cube (BSC2) and measured individually, selected with a flip mirror (FM2). The detection system consists of an infrared filter (F1), a monochromator (MC)(Horiba), and a photomultiplier tube (PMT) (Hamamatsu). The control of the monochromator and the measurements with the PMT were automated using an Arduino, which is managed via custom computer software. The system was benchmarked with a Si(111) sample, and both second- and third-harmonic generation was observed (Figure 9), where we confirmed a scaling factor of  $\sim 2$  and  $\sim 3$ , respectively. We also observed the spectral broadening of the harmonics.



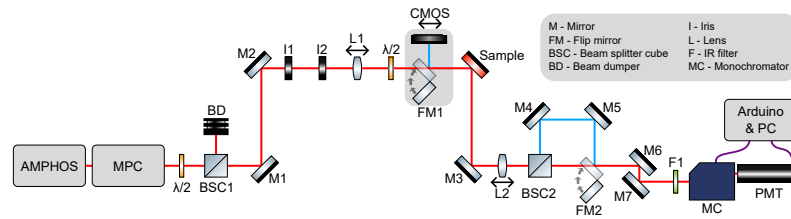


**Figure 8.** Experimental setup for the characterization of the surface nonlinear response of materials.

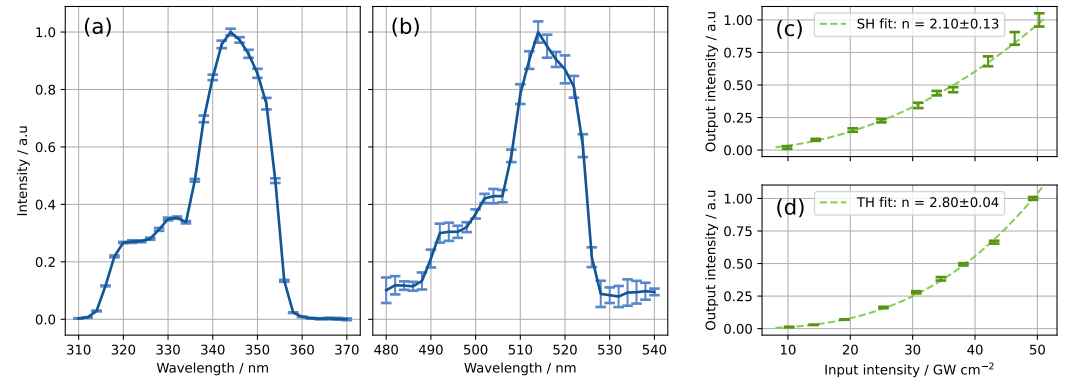


**Figure 9.** Spectrum of the (a) third harmonic with a peak at 344 nm, and (b) second harmonic with a peak at 514 nm. Power scaling for (c) the second harmonic, and (d) the third harmonic.

### 3.1.2. Time-Resolved Infrared Spectroscopy

Time-resolved infrared (TRIR) spectroscopy, a type of ultrafast transient absorption spectroscopy, utilizes a pump–probe geometry to explore molecular dynamics. In this technique, a pump pulse excites a fraction of the molecules in the sample, while the temporal evolution of this excited state is monitored using an infrared probe pulse delayed with respect to the pump. To prevent unwanted multiphoton or multistep processes, the probe pulse is kept at a relatively low intensity.

Our goal is to establish and benchmark a TRIR spectroscopy workstation at the L2I. As a proof of principle, initial tests are being conducted using rhodamine 6G, with the 1030 nm laser from the MPC serving as the pump and its second harmonic at 515 nm, generated in a BBO crystal, as the probe (Figure 10). The advantage of using the MPC output are the shorter pulse durations, contributing to a higher temporal resolution of the system. So far, we have demonstrated time delays up to 2 ns and with a resolution of 1.69 ps using uncompressed pulses. Using the MPC to operate on the 100 fs time scale, we expect a temporal resolution of around 140 fs.

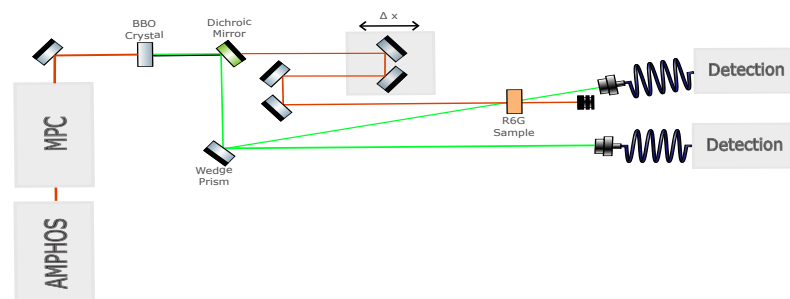


**Figure 10.** Schematic of the experimental setup for transient absorption spectroscopy. The setup utilizes a pump–probe geometry, with the time delay controlled via a translation stage. Detection is carried out by measuring both the probe pulse and a reference pulse which are separated in a wedge.

### 3.2. Mid-Infrared Studies

The 3 μm output from the mid-infrared OPCPA opens the door to the study of new phenomena that cannot be observed in the near-infrared. Below, we provide a few examples of experiments that have been conducted using this system.

#### 3.2.1. Visible Spectral Wings by Supercontinuum Generation

Most materials demonstrate normal dispersion in the visible and near-infrared, but anomalous dispersion for longer wavelengths. During spectral broadening, self-phase modulation combined with anomalous dispersion can lead to self-compression, potentiating larger spectra than those generated in normal dispersion [25].

We used the 3000 nm pulses to drive supercontinuum generation that included isolated spectral wings in the visible and near-infrared range [26]. Figure 11 shows a selection of these wings. This phenomenon associated with the anomalous dispersion regime was also reported in Refs. [27–29].

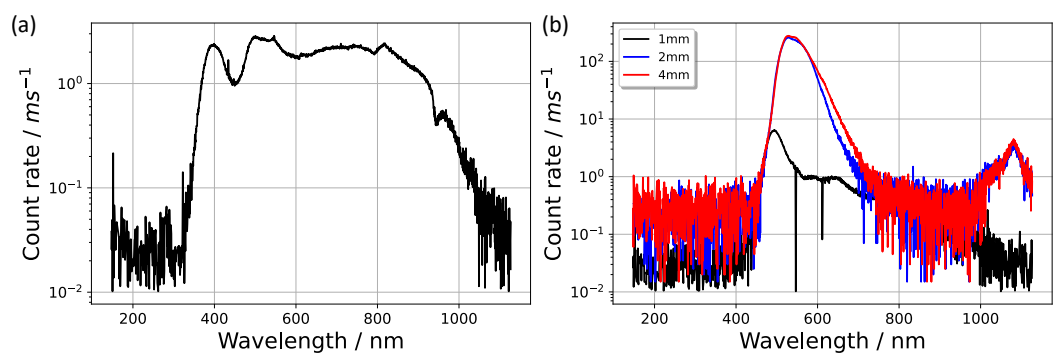


**Figure 11.** Visible spectral wing of supercontinuum generated in (a) 3 mm calcium fluoride and (b) YAG windows with the respective length in the legend. Spectra expressed in count rate of the spectrometer (Sarspec). From Ref. [26].

#### 3.2.2. Harmonic Generation in Solids

The generation of harmonics in solids in the mid-infrared is of particular importance, as driving harmonics at higher wavelengths imposes lower damage thresholds as well as a higher absorption of the high energy harmonics [30,31]. In fact, the first observation of high harmonics in bulk was performed with a 3.25 μm laser [30].

Figures 12 and 13 show a selection of harmonics generated in proof-of-principle experiments using standard samples [26]. Figure 12 shows the observed harmonics in a 1 mm thick sample of calcium fluoride, where we reached up to the ninth order. In thicker samples, we observed the existence of spectral fringes (Figure 13), which are related to the generation of two second-harmonic components propagating at different group velocities due to phase mismatch [32,33]. The experimental fringe spacing  $\Delta\lambda$  is in good agreement with the theoretical values given by [34,35]

$$\Delta\lambda_{theo} = \frac{\lambda_H^2}{d(n_g(\lambda_0) - n_g(\lambda_H))}, \tag{1}$$

where  $\lambda_0 = 3 \mu\text{m}$  is the central wavelength of the fundamental,  $\lambda_H$  is the central wavelength of the harmonic,  $d$  is the sample’s thickness, and  $n_g(\lambda) = n(\lambda) - \lambda \frac{dn(\lambda)}{d\lambda}$  is the group index of the sample for the wavelength  $\lambda$ . The refractive index of the medium,  $n(\lambda)$ , was obtained from the Sellmeier equations [36].

A more in-depth set of experiments were performed with thin samples of  $\beta$ -gallium oxide with different doping levels. These generated both odd and even harmonics up to the ninth order, and we also observed fringe generation as well as high anisotropic polarization response. These results were integrated in a collaborative work which used multiple lasers sources to study this material [35].

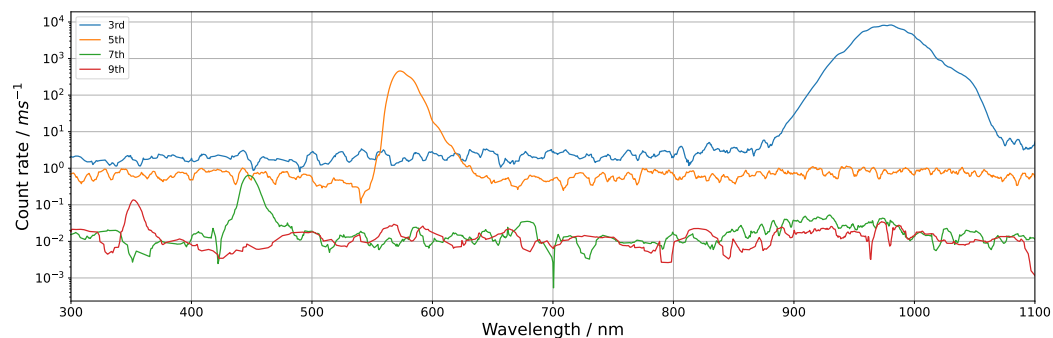


**Figure 12.** Smoothed spectra of all harmonics obtained with a calcium fluoride sample of 1 mm. Spectra expressed in count rate of the spectrometer (Sarspec). From Ref. [26].

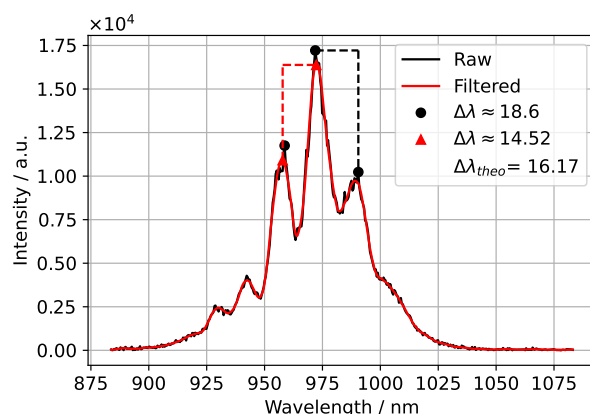


**Figure 13.** Smoothed spectra of the third harmonic with spectral fringes, obtained by propagation in a C-cut sapphire sample of 2 mm.  $\Delta\lambda$  was calculated for the raw data and a smoothed/filtered version to reduce the effect of noise. From Ref. [26].

#### 4. Discussion

The experiments presented in the previous section showcase the feasibility of exploring several scientific fields driven by a single laser source. Currently, we are in the process of preparing and acquiring further samples for more detailed studies, as well as developing additional experimental stations for further applications.

#### 5. Conclusions

The development of the triple-chained OPA is challenging due to limited pulse energy in the mid-IR laser system, currently being addressed by using a homebuilt multipass to amplify them to the multi-mJ level, as the cost of a much lower repetition rate. A more complete solution is possible via thin-disk laser technologies,  $\sim 100$  mJ pulses  $> \text{kHz}$ ; however, this leads to a much higher cost for us when compared to adapting a pre-existing setup.

Regarding the YCOB OPCPA system, the main difficulty is to assure the stability of the cascading nonlinear processes (MPC followed by OPA). These have been carefully monitored and mitigated, but closer to the completion of the systems, passive (operation in a saturation regime) and active approaches (motorized controls of mirrors and attenuators) will be put in place.

In conclusion, we have described the current and planned capabilities of L2I, with special attention to the potential of combining new-generation laser sources with nonlinear stages for the development of a multidisciplinary laser facility. The diversity of pulse parameters enables the performance of experiments in a variety of scientific areas covering a broad range of wavelengths, energies, and pulse durations.

**Author Contributions:** Conceptualization, H.P. and G.F.; formal analysis and investigation, G.V., J.A., V.H., C.P.J., J.M., D.C., H.G., C.P., P.P. and H.P.; writing—original draft preparation, G.V.; writing—review and editing, G.V., H.P. and G.F.; visualization, G.V., J.A., V.H., C.P.J., J.M., D.C., H.G., C.P., P.P. and M.P.S.; supervision, H.P. and G.F.; project administration, H.P. and G.F.; funding acquisition, H.P. and G.F. All authors have read and agreed to the published version of the manuscript.

**Funding:** IPFN activities were supported by FCT—Fundação para a Ciência e Tecnologia, I.P. by project reference UIDB/50010/2020 and DOI identifier 10.54499/UIDB/50010/2020 (<https://doi.org/10.54499/UIDB/50010/2020>), by project reference UIDP/50010/2020 and DOI identifier DOI 10.54499/UIDP/50010/2020 (<https://doi.org/10.54499/UIDP/50010/2020>), and by project reference LA/P/0061/2020 and DOI 10.54499/LA/P/0061/2020 (<https://doi.org/10.54499/LA/P/0061/2020>). This work has received funding from the Fundação para a Ciência e Tecnologia under grant Laserlab Portugal (National Roadmap of Research Infrastructures, PINFRA/22124/2016); and the European Union’s Horizon 2020 research and innovation programme under grant agreement no. 871124 Laserlab-Europe. This work was carried out in the framework of the Advanced Program in Plasma Science and Engineering (sponsored by the Fundação para a Ciência e Tecnologia under grant No. UI/BD/153733/2022).

**Data Availability Statement:** The datasets presented in this article are not readily available because the data are part of an ongoing study. Requests to access the datasets should be directed to hugo.pires@tecnico.ulisboa.pt.

**Conflicts of Interest:** Joana Alves is employed by NKT Photonics A/S; Celso P. João is employed by LaserLeap Technologies. The authors declare that they have no known competing financial interests or personal relationships that could have appeared to influence the work reported in this paper.

## Abbreviations

The following abbreviations are used in this manuscript:

CPA	Chirped Pulse Amplifier
FROG	Frequency-Resolved Optical Gating
L2I	Laboratory of Intense Lasers
MPC	Multipass cell
NOPA	Noncolinear Optical Parametric Amplifier
OPCPA	Optical Parametric Chirped Pulse Amplifier
SPM	Self-phase modulation
TRIR	Time-resolved infrared
YCOB	Yttrium calcium oxyborate

## References

1. Maine, P.; Strickland, D.; Bado, P.; Pessot, M.; Mourou, G. Generation of ultrahigh peak power pulses by chirped pulse amplification. *IEEE J. Quantum Electron.* **1988**, *24*, 398–403. [[CrossRef](#)]
2. Dubietis, A.; Jonušauskas, G.; Piskarskas, A. Powerful femtosecond pulse generation by chirped and stretched pulse parametric amplification in BBO crystal. *Opt. Commun.* **1992**, *88*, 437–440. [[CrossRef](#)]
3. Ross, I.; Matousek, P.; Towrie, M.; Langley, A.; Collier, J. The prospects for ultrashort pulse duration and ultrahigh intensity using optical parametric chirped pulse amplifiers. *Opt. Commun.* **1997**, *144*, 125–133. [[CrossRef](#)]
4. Witte, S.; Eikema, K.S.E. Ultrafast Optical Parametric Chirped-Pulse Amplification. *IEEE J. Sel. Top. Quantum Electron.* **2012**, *18*, 296–307. [[CrossRef](#)]
5. Reid, D.T.; Heyl, C.M.; Thomson, R.R.; Trebino, R.; Steinmeyer, G.; Fielding, H.H.; Holzwarth, R.; Zhang, Z.; Del’Haye, P.; Südmeyer, T.; et al. Roadmap on ultrafast optics. *J. Opt.* **2016**, *18*, 093006. [[CrossRef](#)]
6. Fattahi, H.; Barros, H.G.; Gorjan, M.; Nubbemeyer, T.; Alsaif, B.; Teisset, C.Y.; Schultze, M.; Prinz, S.; Haefner, M.; Ueffing, M.; et al. Third-generation femtosecond technology. *Optica* **2014**, *1*, 45–63. [[CrossRef](#)]
7. Figueira, G.; Alves, J.; Dias, J.M.; Fajardo, M.; Gomes, N.; Hariton, V.; Imran, T.; João, C.P.; Koliyadu, J.; Künzel, S.; et al. Ultrashort pulse capability at the L2I high intensity laser facility. *High Power Laser Sci. Eng.* **2017**, *5*, e2. [[CrossRef](#)]
8. Thiré, N.; Maksimenka, R.; Kiss, B.; Ferchaud, C.; Bizouard, P.; Cormier, E.; Osvay, K.; Forget, N. 4-W, 100-kHz, few-cycle mid-infrared source with sub-100-mrad carrier-envelope phase noise. *Opt. Express* **2017**, *25*, 1505. [[CrossRef](#)]
9. Pires, H.; Baudisch, M.; Sanchez, D.; Hemmer, M.; Biegert, J. Ultrashort pulse generation in the mid-IR. *Prog. Quantum Electron.* **2015**, *43*, 1–30. [[CrossRef](#)]
10. Ma, J.; Qin, Z.; Xie, G.; Qian, L.; Tang, D. Review of mid-infrared mode-locked laser sources in the 2.0  $\mu\text{m}$ –3.5  $\mu\text{m}$  spectral region. *Appl. Phys. Rev.* **2019**, *6*, 021317. [[CrossRef](#)]

11. Hanna, M.; Guichard, F.; Daher, N.; Bournet, Q.; Délen, X.; Georges, P. Nonlinear Optics in Multipass Cells. *Laser Photon. Rev.* **2021**, *15*, 2100220. [[CrossRef](#)]
12. Viotti, A.L.; Seidel, M.; Escoto, E.; Rajhans, S.; Leemans, W.P.; Hartl, I.; Heyl, C.M. Multi-pass cells for post-compression of ultrashort laser pulses. *Optica* **2022**, *9*, 197–216. [[CrossRef](#)]
13. Nagy, T.; Simon, P.; Veisz, L. High-energy few-cycle pulses: Post-compression techniques. *Adv. Phys. X* **2021**, *6*, 1845795. [[CrossRef](#)]
14. Hariton, V. Nonlinear Spectral Broadening and Pulse Compression in Multipass Cells. Ph.D. Thesis, Instituto Superior Técnico, Universidade de Lisboa, Lisbon, Portugal, 2023.
15. Paiva João, C. Diode-Pumped Solid-State Lasers for Optical Parametric Amplification Pumping. Ph.D. Thesis, Instituto Superior Técnico, Universidade de Lisboa, Lisbon, Portugal, 2016.
16. Alves, J.; Pires, H.; João, C.P.; Figueira, G. Multi-mJ Scaling of 5-Optical Cycle, 3  $\mu\text{m}$  OPCPA. *Photonics* **2021**, *8*, 503. [[CrossRef](#)]
17. Alves, J. Ultrafast Mid-Infrared Tunable Laser Sources. Ph.D. Thesis, Instituto Superior Técnico, Universidade de Lisboa, Lisbon, Portugal, 2023.
18. Pires, H.; Galimberti, M.; Figueira, G. Numerical evaluation of ultrabroadband parametric amplification in YCOB. *J. Opt. Soc. Am. B* **2014**, *31*, 2608. [[CrossRef](#)]
19. Galletti, M.; Pires, H.; Hariton, V.; Alves, J.; Oliveira, P.; Galimberti, M.; Figueira, G. Ultra-broadband near-infrared NOPAs based on the nonlinear crystals BiBO and YCOB. *High Power Laser Sci. Eng.* **2020**, *8*, e29. [[CrossRef](#)]
20. Pires, H.; Alves, J.; Hariton, V.; Galletti, M.; João, C.; Figueira, G. Ultrabroadband OPA in YCOB with a sub-ps Pump Source. *Photonics* **2023**, *10*, 253. [[CrossRef](#)]
21. Pires, H. Intense Ultra-Short Laser Pulse Generation. Ph.D. Thesis, Instituto Superior Técnico, Universidade de Lisboa, Lisbon, Portugal, 2015.
22. Hardhienata, H.; Prylepa, A.; Stifter, D.; Hingerl, K. Simplified bond-hyperpolarizability model of second-harmonic-generation in Si(111): Theory and experiment. *J. Phys. Conf. Ser.* **2013**, *423*, 012046. [[CrossRef](#)]
23. Cazzanelli, M.; Schilling, J. Second order optical nonlinearity in silicon by symmetry breaking. *Appl. Phys. Rev.* **2016**, *3*, 011104. [[CrossRef](#)]
24. Tom, H.W.K.; Heinz, T.F.; Shen, Y.R. Second-Harmonic Reflection from Silicon Surfaces and Its Relation to Structural Symmetry. *Phys. Rev. Lett.* **1983**, *51*, 1983–1986. [[CrossRef](#)]
25. Dubietis, A.; Tamošauskas, G.; Šuminas, R.; Jukna, V.; Couairon, A. Ultrafast supercontinuum generation in bulk condensed media. *Lith. J. Phys.* **2017**, *57*, 113–157. [[CrossRef](#)]
26. Vaz, G. Nonlinear Optics with Ultrashort Mid-Infrared Laser Pulses. Master's Thesis, Instituto Superior Técnico, Universidade de Lisboa, Lisbon, Portugal, 2021.
27. Durand, M.; Lim, K.; Jukna, V.; McKee, E.; Baudalet, M.; Houard, A.; Richardson, M.; Mysyrowicz, A.; Couairon, A. Blueshifted continuum peaks from filamentation in the anomalous dispersion regime. *Phys. Rev. A* **2013**, *87*, 043820. [[CrossRef](#)]
28. Dharmadhikari, J.A.; Deshpande, R.A.; Nath, A.; Dota, K.; Mathur, D.; Dharmadhikari, A.K. Effect of group velocity dispersion on supercontinuum generation and filamentation in transparent solids. *Appl. Phys. B* **2014**, *117*, 471–479. [[CrossRef](#)]
29. Smetanina, E.O.; Kompanets, V.O.; Chekalin, S.V.; Dormidonov, A.E.; Kandidov, V.P. Anti-Stokes wing of femtosecond laser filament supercontinuum in fused silica. *Opt. Lett.* **2013**, *38*, 16. [[CrossRef](#)] [[PubMed](#)]
30. Ghimire, S.; DiChiara, A.D.; Sistrunk, E.; Agostini, P.; DiMauro, L.F.; Reis, D.A. Observation of high-order harmonic generation in a bulk crystal. *Nat. Phys.* **2011**, *7*, 138–141. [[CrossRef](#)]
31. Ghimire, S.; Reis, D.A. High-harmonic generation from solids. *Nat. Phys.* **2019**, *15*, 10–16. [[CrossRef](#)]
32. Garejev, N.; Gražulevičiūtė, I.; Majus, D.; Tamošauskas, G.; Jukna, V.; Couairon, A.; Dubietis, A. Third- and fifth-harmonic generation in transparent solids with few-optical-cycle midinfrared pulses. *Phys. Rev. A* **2014**, *89*, 033846. [[CrossRef](#)]
33. Roppo, V.; Centini, M.; Sibilina, C.; Bertolotti, M.; de Ceglia, D.; Scalora, M.; Akozbek, N.; Bloemer, M.J.; Haus, J.W.; Kosareva, O.G.; et al. Role of phase matching in pulsed second-harmonic generation: Walk-off and phase-locked twin pulses in negative-index media. *Phys. Rev. A* **2007**, *76*, 033829. [[CrossRef](#)]
34. Franz, D. High Harmonic Generation in Crystals Assisted by Local Field Enhancement in Nanostructures. Ph.D. Thesis, Université Paris Saclay (COMUE), Paris, France, 2018.
35. Hussain, M.; Antunes, A.M.; Vaz, G.; Alves, J.; Pires, H.; Imran, T.; Peres, M.; Lorenz, K.; Villora, E.; Shimamura, K.; et al. Anisotropic below bandgap harmonic generation in  $\beta$ -gallium oxide. *Opt. Express* **2024**. [[CrossRef](#)]
36. Dodge, M.J. *Handbook of Laser Science and Technology, Volume IV, Optical Materials: Part 2*; CRC Press: Boca Raton, FL, USA, 1986; Chapter Refractive Index, p. 30.

**Disclaimer/Publisher's Note:** The statements, opinions and data contained in all publications are solely those of the individual author(s) and contributor(s) and not of MDPI and/or the editor(s). MDPI and/or the editor(s) disclaim responsibility for any injury to people or property resulting from any ideas, methods, instructions or products referred to in the content.